



## Elaboration of strontium apatites doped with lanthanum and cesium by solid-state reaction and by mechanochemical synthesis

Nadia Gmati<sup>1</sup>, Hassan Agougui<sup>2</sup>, Mustapha Hidouri<sup>3</sup>, Khaled Boughzala<sup>4\*</sup>

<sup>1</sup>Process Engineering Department, Higher Institute of Technological Studies, BP 68, Av. Hadj Ali Soua, Ksar Hellal 5070, Monastir, Tunisia

<sup>2</sup>Laboratory of Physical-chemistry of Materials, Faculty of Sciences of Monastir, 5019 Monastir, Tunisia

<sup>3</sup>High Institute of Applied Sciences and Technology, 6072 Zrig, Gabes University, Tunisia

<sup>4</sup>RU Analysis and applied process for Environment, High Institute for Applied Sciences and Technology, 5121 Mahdia, Tunisia

[\\*khaledboughzala@gmail.com](mailto:*khaledboughzala@gmail.com)

Received 07 May 2022,  
Revised 31 May 2022,  
Accepted 02 June 2022

### Keywords

- ✓ Apatite
- ✓ Caesium
- ✓ Solids state reaction,
- ✓ Mechanochemical synthesis,
- ✓ DRX
- ✓ IR.

### Abstract

Fluorbritholites correspond to apatites comprising one or more silicates groups and retaining rare earth elements. These materials are chemically and thermally stable exhibiting thus high ability for the confinement of certain radionuclides like cesium Cs. Herein, lacunal britholites containing cesium were prepared twice by solid-state reaction and mechanochemical synthesis. Three compositions were investigated, Sr<sub>8</sub>LaCs(PO<sub>4</sub>)<sub>6</sub>F<sub>2</sub>, Sr<sub>7</sub>La<sub>2</sub>Cs(PO<sub>4</sub>)<sub>5</sub>(SiO<sub>4</sub>)F<sub>2</sub> and Sr<sub>2</sub>La<sub>7</sub>Cs(SiO<sub>4</sub>)<sub>6</sub>F<sub>2</sub>. The results of X-ray diffraction and infrared spectroscopy analyses showed that it is possible to obtain such apatite by the both synthetic methods. However, there was formation of secondary phases whose nature is closely related to the initial composition....

## 1. Introduction

Apatites belong to a large family of compounds with the general chemical formula  $M_{10}(XO_4)_6Y_2$ , where M represents a divalent cation,  $XO_4$  an anion group and Y a monovalent anion. These materials crystallize mainly in the hexagonal system with the space group P6<sub>3</sub>/m [1]. Owing to their chemical and thermal stability, apatite-type materials have attracted a lot of interest. They are used as bone substitutes in orthopedics and dentistry [2-4], fluorescent lamp phosphors [5, 6], laser host [6], gas sensors [7] or catalysis materials [8]. Physico-chemical properties are modified and affected by a wide range of cationic and anionic substitutions [9-11]. For example, the simultaneous substitutions of La<sup>3+</sup> and SiO<sub>4</sub><sup>4-</sup> by Ca<sup>2+</sup> and PO<sub>4</sub><sup>3-</sup>, result in a new family of compounds called britholites [12, 13]. These compounds are potential candidates for the retention of certain radionuclides [14, 15]. Indeed, the discovery of the Oklo site [16-18] confirmed their ability to retain actinide elements with thermal and chemical stability under radiation conditions. In addition, silicate apatitic compounds have recently emerged as an alternative electrolytic material for solid oxide fuel cells [19-23].

These compounds are usually prepared by solid state reaction at higher temperatures. In addition, several heat treatments are often required to obtain single-phase materials [24-27]. On the contrary, mechano-chemical synthesis involves only a reaction in the solid state at room temperature [28, 29].

Therefore, this method seems quite interesting for the preparation of this type of material [30, 31]. This method was originally developed by Benjamin and his collaborators in the early 1970s [32]. In mechano-chemical synthesis, a mixture of elemental powders is subjected in a mill to successive intense shocks with adjustable frequencies and energies. These shocks by creating point, linear or surface defects induce an increase in the free energy of the initial material. Therefore, to minimize free energy, phases of change and transformation occur in the system leading to the desired product [33, 34].

In this work, we consider the synthesis by solid state reaction and by mechanochemical synthesis of britholites containing cesium, with the general formula  $\text{Sr}_{8-x}\text{La}_{1-x}\text{Cs}(\text{PO}_4)_{6-x}(\text{SiO}_4)_x\text{F}_2$ , with  $x = 0, 1$  and  $6$ . The resulting products were characterized by X-ray diffraction and infrared spectroscopy.

## 2. Experimental protocol

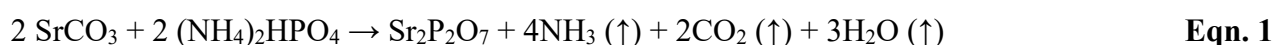
### 2.1 Preparation of powders

Cesium-based britholites were dry-synthesized in two stages from  $\text{SrCO}_3$  (>96% Riedel de Haen),  $\text{La}_2\text{O}_3$  (>99.5% Prolabo),  $\text{SiO}_2$  (>99.5% Alfa),  $\text{SrF}_2$  (>99.5% Prolabo),  $\text{Cs}_2\text{CO}_3$  (>99% Fluka),  $\text{NH}_4\text{F}$  (> 95% Merck) and  $\text{Sr}_2\text{P}_2\text{O}_7$ .

### 2.2 Experiments

#### 2.1.1. Preparation of $\text{Sr}_2\text{P}_2\text{O}_7$

Strontium di-phosphate was obtained according to the following reaction:

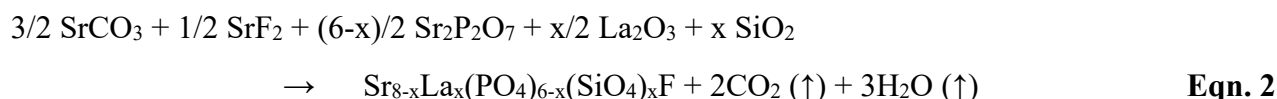


After being crushed and homogenized in an agate mortar, the mixture of strontium carbonate and di-ammonium-hydrogen phosphate was shaped by cold uniaxial pressing and then calcined at  $900^\circ\text{C}$  for 10 hours. The temperature rise and cooling were carried out at a speed of  $10^\circ\text{C}/\text{min}$ .

#### 2.1.2. Solid synthesis of powders

##### 2.1.2.1. Preparation of britholites deficiency

Incomplete britholites of general formula  $\text{Sr}_{8-x}\text{La}_x(\text{PO}_4)_{6-x}(\text{SiO}_4)_x\text{F}$  were prepared according to the following equation:

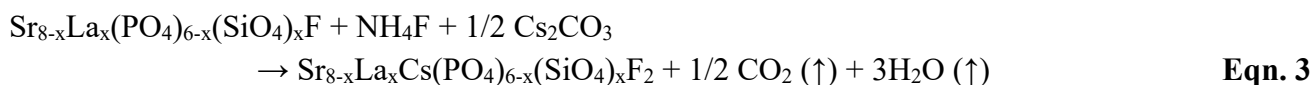


After prolonged manual grinding and homogenization of the reagents in an agate mortar, the mixtures were shaped by cold uniaxial pressing. The pellets obtained were treated under dynamic argon atmosphere at  $900^\circ\text{C}$  for 12 hours to carry out their degassing, then, after a new grinding / homogenization step, a heat treatment of 12 hours at  $1400^\circ\text{C}$  was applied.

##### 2.1.2.2. Preparation of cesium-doped britholites

The lacunar britholites obtained were mixed with cesium carbonate ( $\text{Cs}_2\text{CO}_3$ ) and ammonium fluoride ( $\text{NH}_4\text{F}$ ), crushed and compacted according to the previous operating protocol. After a first treatment at  $800^\circ\text{C}$  for 2 hours, the pellets obtained were again crushed, homogenized and shaped.

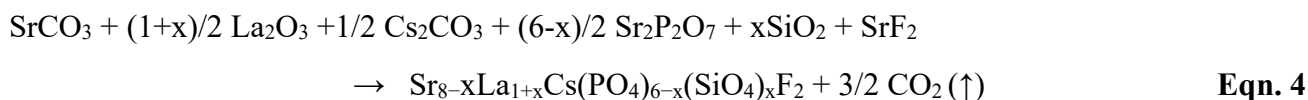
In order to limit the volatilization of cesium [24, 25], the pellets were placed in a basket with a lid, coated with a powder of the same nature, but enriched with cesium carbonate (20% by mass), to create a self-stabilizing atmosphere. They were then calcined at 1100 °C for 4 hours. The reaction is as follows:



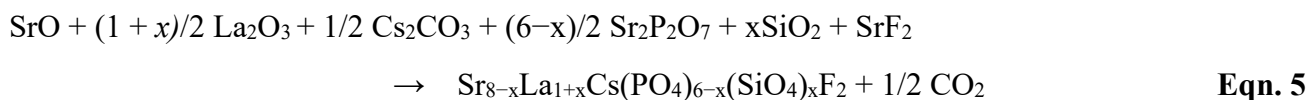
### 2.1.2. Synthesis of powders by mechanosynthesis

The apatites, containing cesium of general formula  $\text{Sr}_{8-x}\text{La}_{1+x}\text{Cs}(\text{PO}_4)_{6-x}(\text{SiO}_4)_x\text{F}_2$  with  $x = 0, 1$  and 6, were prepared according to two different protocols.

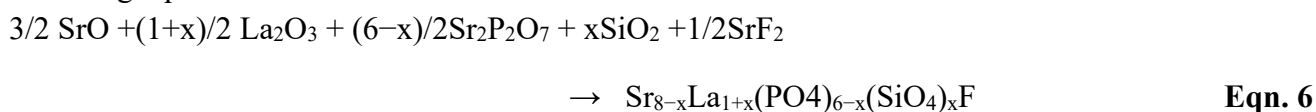
According to the first procedure, the grinding of the reagents was carried out in a single step using, i.e. strontium carbonate:



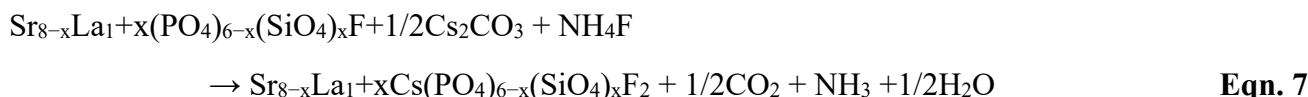
With strontium oxide:



In the second procedure, intermediate apatitic phases, with general formula  $\text{Sr}_{8-x}\text{La}_{1+x}(\text{PO}_4)_{6-x}(\text{SiO}_4)_x\text{F}$ , with  $x = 0, 1$  and 6, were prepared, in a first step, according to the following equation:



Then, in a second step, cesium carbonate and ammonium fluoride were added to the phases previously obtained according to the following equation:



In this method, the reactants taken in stoichiometric proportions were introduced into a 45 cm<sup>3</sup> jar containing five balls of 12 mm in diameter. The jar and balls are made of steel. The mass ratio of the balls to the mass of the powder is 34/1. The rotational speeds of the tray and the jar were equal to 500 and 1000 rpm respectively. These operating conditions correspond to a shock kinetic energy of 0.151 J/shock, a shock frequency of 100 Hz and an injected shock power of 15.1 W/g. The samples were crushed for periods of between 30 minutes and 25 hours. The preparation of these compounds was carried out in a planetary mill of the Retsch PM 200 type. The various samples were also calcined at 900°C and 1100°C under a dynamic argon atmosphere. The duration of each heat treatment was 6 hours. The rate of temperature rise for all heat treatments was 10°C/min.

### 2.3. Characterization of powders

X-ray diffraction (XRD) analysis of the samples was performed using a PANalytical X'Pert Pro diffractometer, using Copper Ka radiation ( $\lambda = 1.5406 \text{ \AA}$ ). The diffractograms were acquired in the range 0-75° in 2θ by step-by-step acquisition at the speed of 0.02 °/s. PANalytical's X'Pert High

Score Plus software was used to identify crystalline phases by comparing the resulting DRX diagrams to the files in the JCDJ PDF-2 database. Infrared spectra were recorded in the 400-4000  $\text{cm}^{-1}$  wavelength range using a Perkin Elmer 1283 Fourier transform spectrometer, using the KBr technique.

### 3. Results and Discussion

#### 3.1 X-ray diffraction

The analysis by DRX of the lacunar samples prepared by dried route reveals the formation of a majority apatitic phase indexed from the JCPDS sheet n° 17-609.

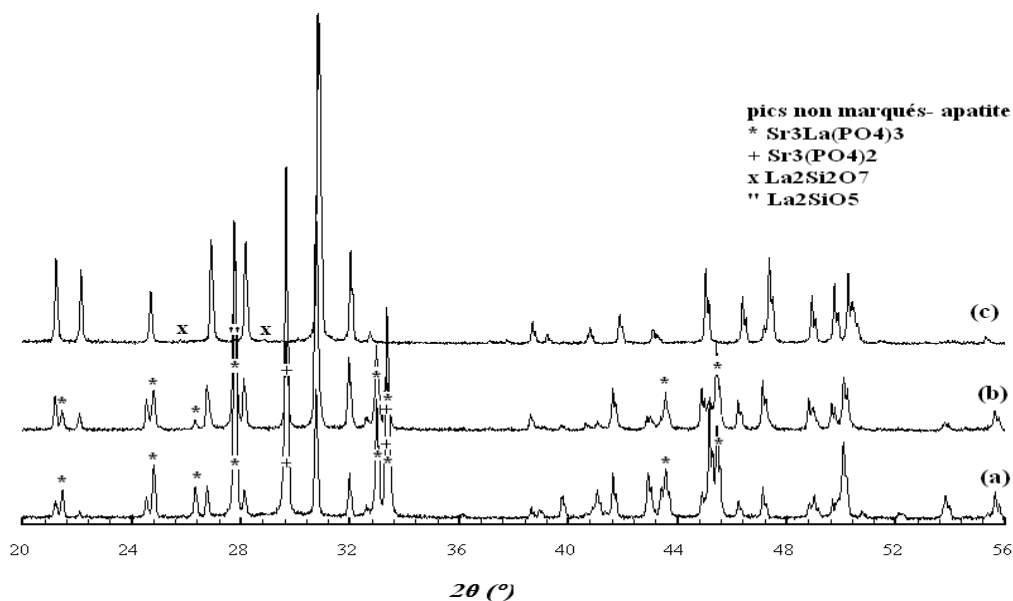
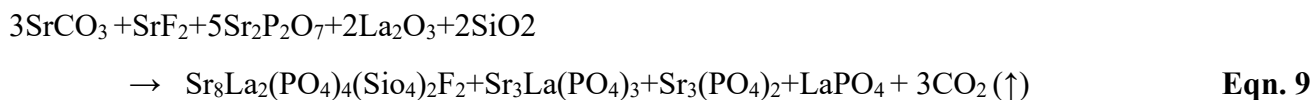
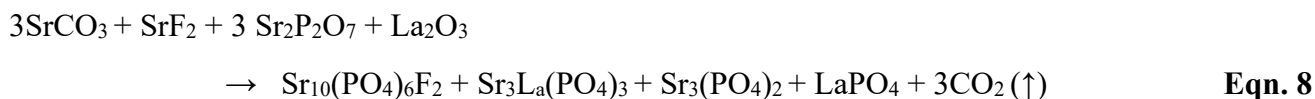


**Figure 1.** DRX diagrams of Britholites lacking compositions: (a)  $\text{Sr}_8\text{La}(\text{PO}_4)_6\text{F}$ , (b)  $\text{Sr}_7\text{La}_2(\text{PO}_4)_5(\text{SiO}_4)\text{F}$  and (c)  $\text{Sr}_2\text{La}_7(\text{SiO}_4)_6\text{F}$ .

In the case of the compositions  $\text{Sr}_8\text{LaF}$  (**Figure 1a**) and  $\text{Sr}_7\text{La}_2\text{F}$  (**Figure 1b**), we note the presence of secondary phases  $\text{Sr}_3\text{La}(\text{PO}_4)_3$  and  $\text{Sr}_3(\text{PO}_4)_2$ , indexed respectively from sheets n° 85-905 and n° 32-493. In the case of the composition  $\text{Sr}_2\text{La}_7\text{F}$  (**Figure 1c**), the secondary phases identified are  $\text{La}_2\text{Si}_2\text{O}_7$  and  $\text{La}_2\text{SiO}_5$ . They correspond respectively to files n° 44-346 and n° 40-234. It is well known that non-stoichiometric apatites are not stable at high temperatures [35], the secondary phases would then be formed respectively according to the following reactions:



The absence of  $\text{LaPO}_4$  can be explained by a formed amount too small to be detected by DRX or by its combination with tristrontium phosphate  $\text{Sr}_3(\text{PO}_4)_2$  according to the following chemical equation:



Eqn. 11

The crystallographic parameters  $a$  and  $c$  of the lacunar apatitic compounds collected in **Table 1** were determined by the least square method. Note that when the number of  $\text{SiO}_4$  groups, increased,  $a$  increases while  $c$  decreases.

**Table 1.** Crystallographic parameters of lacunar and cesium-doped britholites.

Compositions	$a$ (Å)	$c$ (Å)
SrLaF	9,715(5)	7,282(4)
SrLa <sub>2</sub> F	9,725(3)	7,275(4)
Sr <sub>2</sub> La <sub>7</sub> F	9,740(2)	7,260(1)
SrLaCsF <sub>2</sub>	9,729(5)	7,290(5)
SrLa <sub>2</sub> CsF <sub>2</sub>	9,746(1)	7,289(2)
SrLa <sub>7</sub> CsF <sub>2</sub>	9,752(5)	7,270(3)

The DRX diagrams of cesium-doped britholites are shown in **Figure 2**. After cesium incorporation among the three intermediate compositions, only the composition  $\text{Sr}_7\text{La}_2$  allows the obtaining of a pure apatitic phase (**Figure 2b**) of formula  $\text{Sr}_7\text{La}_2\text{Cs}(\text{PO}_4)_5(\text{SiO}_4)\text{F}_2$ . For the composition  $\text{Sr}_8\text{La}$ , there is disappearance of the secondary phases  $\text{Sr}_3\text{La}(\text{PO}_4)_3$  and  $\text{Sr}_3(\text{PO}_4)_2$  and appearance of a new phase  $\text{SrLaCs}(\text{PO}_4)_2$  sheet n° 35-426 (**Figure 2a**). In the case of the purely silicate lacunar phase treated with cesium, the DRX diagram (**Figure 2c**) shows the presence of a majority apatitic phase of formula  $\text{Sr}_2\text{La}_7\text{Cs}(\text{SiO}_4)_6\text{F}_2$  and two new secondary phases  $\text{CsLaSiO}_4$  and  $\text{Sr}_2\text{SiO}_4$ , identified respectively from sheets No. 49-663 and No. 38-271.

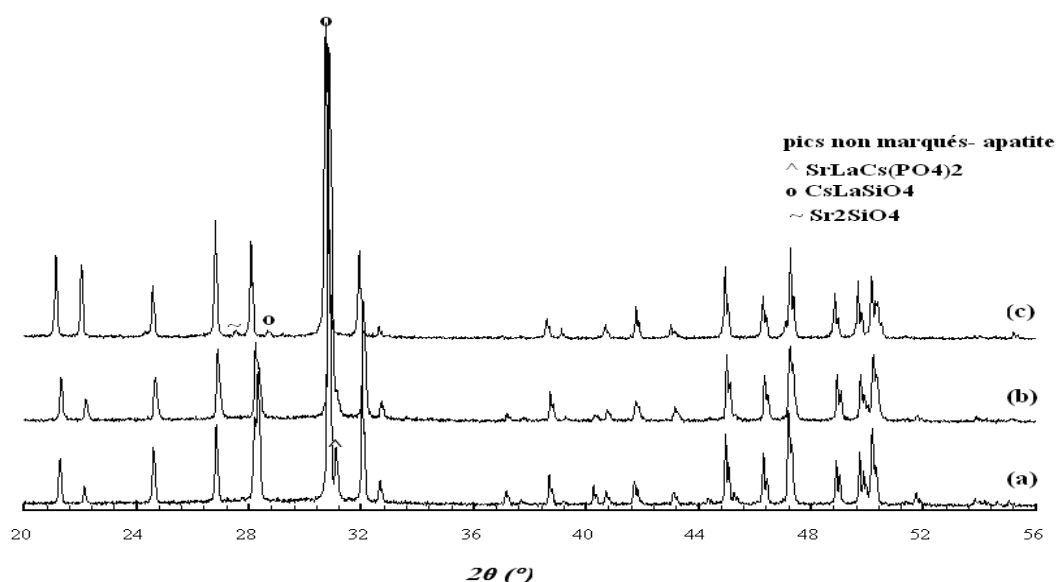


**Figure 2.** DRX diagrams of cesium-doped britholites of compositions: (a)  $\text{Sr}_8\text{LaCs}(\text{PO}_4)_6\text{F}_2$ , (b)  $\text{Sr}_7\text{La}_2\text{Cs}(\text{PO}_4)_5(\text{SiO}_4)\text{F}_2$  and (c)  $\text{Sr}_2\text{La}_7\text{Cs}(\text{SiO}_4)_6\text{F}_2$ .

Also, the incorporation of cesium ( $r_{\text{Cs}^{2+}} = 1.78 \text{ \AA}$ ) [36] in cationic sites and  $\text{F}^-$  ions ( $r_{\text{F}^-} = 1.30 \text{ \AA}$ ) in the anionic gaps of tunnels parallel to the  $c$  axis is accompanied by an increase in parameters  $a$  and  $c$  (**Table 1**). Indeed, according to a Fourier study carried out by Senamaud on britholites substituted for

neodymium, the incorporation of cesium takes place in the cationic sites of apatite. However, its location on the Me(1) or Me(2) site was not possible [35].

Thus, among the three lacunar compositions studied, the composition  $\text{Sr}_7\text{La}_2$  appears as that allowing a better retention of cesium in the apatitic structure since no secondary phase containing this element has been detected. At the same temperature, its calcium analogue and neodymium was obtained mixed with the  $\text{CaNdCs}(\text{PO}_4)_2$  phase, whose formation would be due to the non-stoichiometry of britholite [35]. According to Campayo et al. [37, 38], this  $\text{CaNdCs}(\text{PO}_4)_2$  phase does not appear to be prohibitive to the conditioning of cesium, whereas the secondary phases formed with the phosphate and silicate poles are sufficiently soluble to hinder the use of the latter for the containment of this element.

For samples prepared by mechanosynthesis, the DRX spectra of the three samples prepared in a single step for grinding times between 30 minutes and 20 hours, according to Eqn.4, are shown in Figure 3. The diffractogram of the  $\text{Sr}_8\text{LaCs}$  sample, crushed for 30 minutes Figure 3a, shows the emergence of four new DRX peaks at  $21.99^\circ$ ;  $31.83^\circ$ ;  $38.54^\circ$  and  $42.87^\circ$ , belonging to the apatitic phase. Note that the intensity of the DRX peaks increases with the grinding time, while the intensity of the DRX peaks of the reactants decreases. It should be noted that the majority of reagents disappear after one hour of grinding and that additional diffraction peaks appear. They were assigned to the compounds  $\text{Sr}_3(\text{PO}_4)_2$  and  $\text{SrLaCs}(\text{PO}_4)_2$ , indexed, respectively, from JCPDS sheets no 01-085-0905 and no 00-035-0426. These phases remain present even for grinding times of 25 hours (Figure 3a).

For the  $\text{Sr}_7\text{La}_2\text{Cs}$  sample (Figure 3b), prepared in a single step, the diffractograms of the mixtures crushed for 30 minutes and one hour are virtually identical to those of the  $\text{Sr}_8\text{LaCs}$  sample. For grinding times of between three and five hours, all DRX peaks belong to the apatitic phase. Beyond that, there are new peaks associated with the  $\text{Sr}_3(\text{PO}_4)_2$  and  $\text{SrLaCs}(\text{PO}_4)_2$  phases. The lack of detection of these phases for grinding times between three and five hours is probably due to their small quantities. The diffractograms in Figure 3c corresponding to the  $\text{Sr}_2\text{La}_7\text{Cs}$  sample show that for 30 minutes and one hour of grinding, all the peaks belong to the starting products and that the apatitic phase appears only from three hours. For grinding times equal to or greater than 10 hours, the diffractograms present, in addition to those of apatite, new peaks corresponding to the secondary phases  $\text{La}_2\text{Si}_2\text{O}_7$  and  $\text{CsLaSiO}_4$ , indexed from the JCPDS sheets no 00-048-0052 and no 00-049-0663. It should be noted that silica remains present until a grinding time of 15 hours. This unincorporated silica was replaced in the apatitic structure by carbonates from the reactants, which were detected by infrared spectroscopy.

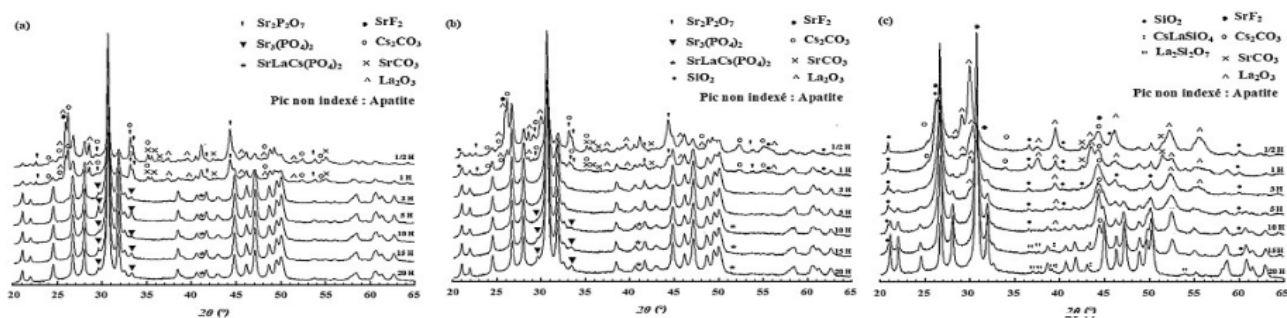


**Figure 3.** X-ray diffraction spectra of samples prepared according to Eqn.4:

(a):  $\text{Sr}_8\text{LaCs}$ ; (b):  $\text{Sr}_7\text{La}_2\text{Cs}$ ; (c):  $\text{Sr}_2\text{La}_7\text{Cs}$ .

In order to minimize the amount of carbonates incorporated into the apatitic structure, we carried out experiments using SrO instead of SrCO<sub>3</sub>, using the same experimental protocol as before. The DRX spectra of the three samples crushed for 25 hours (**Figure 4**) show that there is formation of the same phases as those observed using SrCO<sub>3</sub>.

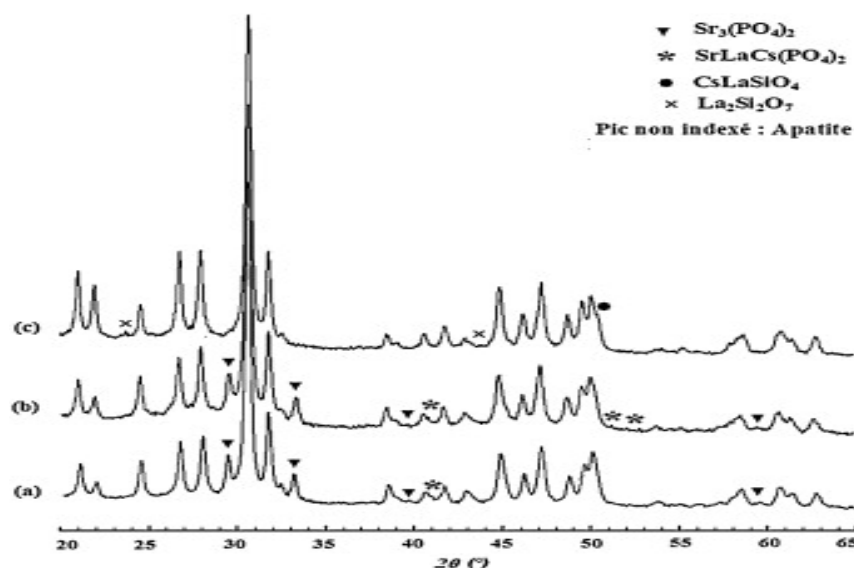
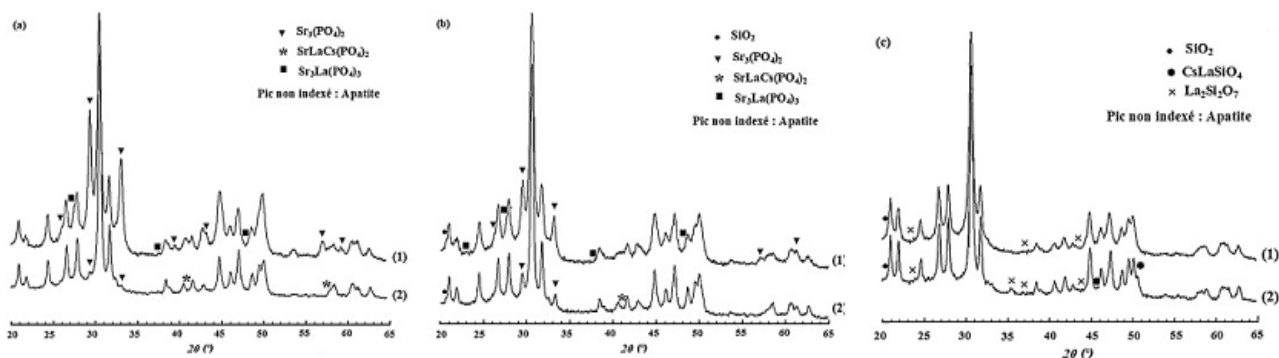


Figure 4. X-ray diffraction spectra of samples prepared according to Eqn.5 :  
**(a)** : Sr<sub>8</sub>LaCs ; **(b)**: Sr<sub>7</sub>La<sub>2</sub>Cs; **(c)**: Sr<sub>2</sub>La<sub>7</sub>Cs.

Similarly, we wanted to verify the influence of the operating procedure on the nature of the products formed. To do this, we used the experimental protocol recommended in the synthesis of cesium apatites by reaction to the solid state at high temperature, that is to say by preparing, before the incorporation of cesium, intermediate apatitic phases (**Eqn. 6**) [39]. **Figure 5** shows the DRX spectra of apatites before and after incorporation of cesium, crushed, respectively, for 25 hours. For the intermediate phases of formula  $Sr_{8-x}La_{1+x}(PO_4)_{6-x}(SiO_4)_x F$  with  $x = 0$  and  $1$ , the diffractograms reveal, in addition to that of apatite, the formation of Sr<sub>3</sub>(PO<sub>4</sub>)<sub>2</sub> and Sr<sub>3</sub>La(PO<sub>4</sub>)<sub>3</sub> (**Figure 5a -b**). For  $x = 6$ , the phase formed in addition to apatite is La<sub>2</sub>Si<sub>2</sub>O<sub>7</sub> (**Figure 5c**). After incorporation of cesium, the detected phases are the same as those observed after grinding in a single step.



**Figure 5.** X-ray diffraction spectra of samples prepared in two stages: **(a)**: Sr<sub>8</sub>LaCs; **(b)**: Sr<sub>7</sub>La<sub>2</sub>Cs; **(c)** :Sr<sub>2</sub>La<sub>7</sub>Cs: **(1)**: intermediate apatites (**Eqn. 6**); **(2)**: apatites doped with cesium **Eqn. 7**.

**Table 2** presents the phases formed during the preparation of samples by mechanosynthesis (present work) and by high temperature reaction [40].

**Table 2.** Products formed by mechanosynthesis (present work) and by high temperature reaction [42]

	Mechanochemical	High temperature reaction	
		Step 1	Step 2
<b>Sr<sub>8</sub>LaCs</b>	Apatite	Apatite	Apatite
	Sr <sub>3</sub> (PO <sub>4</sub> ) <sub>2</sub>	Sr <sub>3</sub> La(PO <sub>4</sub> ) <sub>3</sub>	SrLaCs(PO <sub>4</sub> ) <sub>2</sub>
	SrLaCs(PO <sub>4</sub> ) <sub>2</sub>	Sr <sub>3</sub> (PO <sub>4</sub> ) <sub>2</sub>	
<b>Sr<sub>7</sub>La<sub>2</sub>Cs</b>	Apatite	Apatite	Apatite
	Sr <sub>3</sub> (PO <sub>4</sub> ) <sub>2</sub>	Sr <sub>3</sub> La(PO <sub>4</sub> ) <sub>3</sub>	SrLaCs(PO <sub>4</sub> ) <sub>2</sub>
	SrLaCs(PO <sub>4</sub> ) <sub>2</sub>	Sr <sub>3</sub> (PO <sub>4</sub> ) <sub>2</sub>	
<b>Sr<sub>2</sub>La<sub>7</sub>Cs</b>	Apatite	Apatite	Apatite
	La <sub>2</sub> Si <sub>2</sub> O <sub>7</sub>	La <sub>2</sub> Si <sub>2</sub> O <sub>7</sub>	Sr <sub>2</sub> SiO <sub>4</sub>
	CsLaSiO <sub>4</sub>	La <sub>2</sub> SiO <sub>5</sub>	CsLaSiO <sub>4</sub>

This table shows that the synthesis method adopted influences the phases formed after reaction. Samples prepared by high temperature reaction showed that in addition to apatite, the presence of the SrLaCs(PO<sub>4</sub>)<sub>2</sub> phase, for  $x = 0$  and 1, and the CsLaSiO<sub>4</sub> and Sr<sub>2</sub>SiO<sub>4</sub> phases, for  $x = 6$  [40]. On the other hand, by mechanosynthesis, whether the preparation is carried out in one or two steps, for the first two samples, tri-structic phosphate was detected in addition to apatite and SrLaCs(PO<sub>4</sub>)<sub>2</sub>, while in the case of the third sample, the secondary phases are CsLaSiO<sub>4</sub> and La<sub>2</sub>Si<sub>2</sub>O<sub>7</sub>. Thus, according to the DRX analysis, the only phases containing cesium that have been formally detected are SrLaCs(PO<sub>4</sub>)<sub>2</sub> ( $x = 0$  and 1) and CsLaSiO<sub>4</sub> ( $x = 6$ ). At this stage, the incorporation of this element into the apatitic structure cannot be affirmed with certainty. Also, if this insertion has actually taken place, the quantity inserted is necessarily lower than that introduced into the initial mixture. The mesh parameters of the samples prepared with SrCO<sub>3</sub> and SrO were calculated using the least squares method (Table 3).

**Table 3.** Unit cell parameters of the apatites obtained using SrCO<sub>3</sub> and SrO after a grinding of 25 hours.

Samples		$a = b$ (Å)	$c$ (Å)	$V$ (Å <sup>3</sup> )
<b>Sr<sub>8</sub>LaCs</b>	SrCO <sub>3</sub>	9,726(4)	7,288(3)	597,718(3)
	Ors	9,728(5)	7,287(4)	597,881(4)
<b>Sr<sub>7</sub>La<sub>2</sub>Cs</b>	SrCO <sub>3</sub>	9,730(3)	7,285(4)	597,963(3)
	Ors	9,739(5)	7,287(4)	599,234(4)
<b>Sr<sub>2</sub>La<sub>7</sub>Cs</b>	SrCO <sub>3</sub>	9,747(2)	7,277(3)	599,395(2)
	Ors	9,751(3)	7,270(2)	599,310(2)

The interpretation of the evolution of parameters with substitution remains difficult because of the different sizes of the ions in substitution (Table 4) [36]. However, some conclusions can be drawn. Regardless of the reagent used, the parameter  $a$  increases, while  $c$  decreases. This decrease is even very small. As is also expected, the mesh parameters of apatites prepared with SrCO<sub>3</sub> are lower than those of apatites obtained with SrO, since the latter normally contain less carbonate.

**Table 4.** Ionic radius of substituting ions.

Ions	Sr <sup>2+</sup>	The <sup>3+</sup>	Cs <sup>+</sup>	P <sup>5+</sup>	Si <sup>4+</sup>	C <sup>4+</sup>
Coordination	9	9	9	4	4	4
Ion rays (Å)	1,31	1,22	1,78	0,17	0,26	0,15

In addition, the incorporation of cesium into apatite must be accompanied by a significant increase in mesh volume. **Table 5** shows that the parameters of intermediate apatites are lower than those of apatites containing cesium. This suggests that some of this element has been incorporated into the apatitic structure.

**Table 5.** Unit cell parameters of intermediate apatites.

Samples	<i>a</i> (Å)	<i>c</i> (Å)	V (Å <sup>3</sup> )
Sr <sub>8</sub> LaF	9,713(3)	7,281(4)	595,548(3)
Sr <sub>7</sub> La <sub>2</sub> F	9,726 (5)	7,279(5)	596,979(5)
Sr <sub>2</sub> La <sub>7</sub> F	9,738(3)	7,263(5)	597,248(4)

### 3.2 Infrared spectroscopy

The infrared absorption spectra of the lacunar britholites presented in **Figure 6** highlight the presence of the absorption bands of the PO<sub>4</sub> and SiO<sub>4</sub> groups. Their allocation was made by comparison with the spectra of the phases Sr<sub>10</sub>(PO<sub>4</sub>)<sub>6</sub>F<sub>2</sub>, Sr<sub>8</sub>La<sub>2</sub>(PO<sub>4</sub>)<sub>4</sub>(SiO<sub>4</sub>)<sub>2</sub>F<sub>2</sub> and Sr<sub>4</sub>La<sub>6</sub>(SiO<sub>4</sub>)<sub>2</sub>F<sub>2</sub> [41]. The additional bands appearing on some spectra around 3450, 1640 and 1380 cm<sup>-1</sup> would be relative to the surface OH groups due to the rehydration of the powder after synthesis [42].

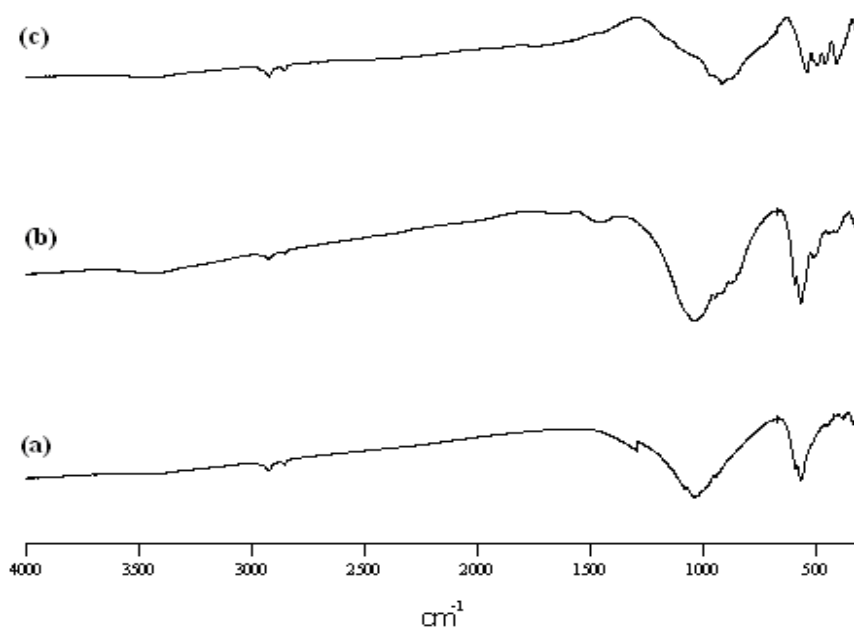


**Figure 6.** Infrared absorption spectra of lacunary britholites (a) Sr<sub>8</sub>La(PO<sub>4</sub>)<sub>6</sub>F, (b) Sr<sub>7</sub>La<sub>2</sub>(PO<sub>4</sub>)<sub>5</sub>(SiO<sub>4</sub>)F and (c) Sr<sub>2</sub>La<sub>7</sub>(SiO<sub>4</sub>)<sub>6</sub>F

**Table 6.** Attribution and positions in  $\text{cm}^{-1}$  of the IR absorption bands of lacunary britholites un- and doped with cesium.

Compositions	$\text{PO}_4^{3-}$				$\text{SiO}_4^{4-}$			
	$\nu_1$ ( $\text{cm}^{-1}$ )	$\nu_2$ ( $\text{cm}^{-1}$ )	$\nu_3$ ( $\text{cm}^{-1}$ )	$\nu_4$ ( $\text{cm}^{-1}$ )	$\nu_1$ ( $\text{cm}^{-1}$ )	$\nu_2$ ( $\text{cm}^{-1}$ )	$\nu_3$ ( $\text{cm}^{-1}$ )	$\nu_4$ ( $\text{cm}^{-1}$ )
SrF	944	450	1082 1038	589 564	-	-	-	-
SrLa <sub>2</sub> F	918 -	509 -	- 1037	594 564	- 870	436 404	- 946	564 -
SrLa <sub>7</sub> F	-	-	-	-	919 848	455 407	- 964 872	542 492
SrLaCsF	942	446	1080 1035	586 560	-	-	-	-
SrLa <sub>2</sub> CsF	912	506	1076 1035	589 560	- 865	432 402	- 942	560 544
SrLa <sub>7</sub> CsF	-	-	-	-	916 846	450 401	1034 956	540 489

The infrared absorption spectra of cesium-doped samples (Figure 7) are similar to those of lacunar britholites. However, a displacement of the absorption bands of the  $\text{PO}_4$  and  $\text{SiO}_4$  groups toward lower wavenumbers (Table 6). This displacement would be due to the expansion of the unit cell [42]. This result corroborates those obtained by X-ray diffraction and confirms the incorporation of cesium into the apatitic lattice. The additional bands previously observed around 3450, 1640 and 1380  $\text{cm}^{-1}$  are also present [42].

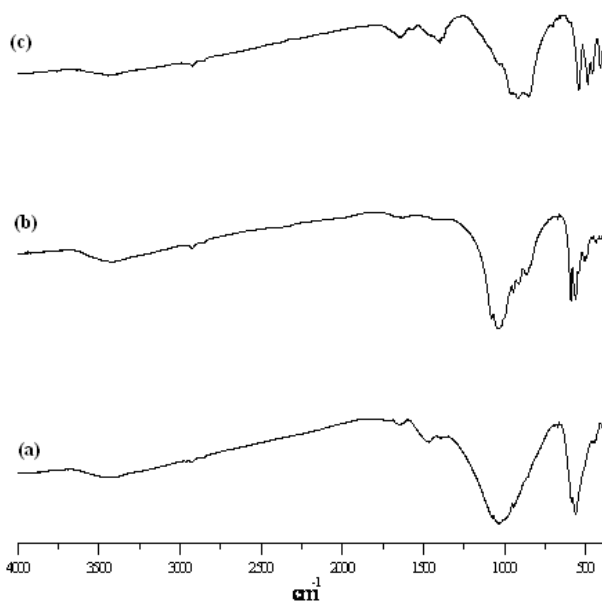


**Figure 7.** Infrared absorption spectra of cesium-doped britholites of compositions: (a)  $\text{Sr}_8\text{LaCs}(\text{PO}_4)_6\text{F}_2$ , (b)  $\text{Sr}_7\text{La}_2(\text{PO}_4)_5(\text{SiO}_4)\text{F}_2$  and (c)  $\text{Sr}_2\text{La}_7(\text{SiO}_4)_6\text{F}_2$ .

**Figure 8** shows the infrared absorption spectra of the compounds obtained by mechanochemical synthesis according to **Eqn. 4**, after grinding to different durations. These spectra show the progress of the formation reaction of the apatitic phase. However, due to the complexity of the system due to the reagents used, the allocation of the observed bands was sometimes difficult. For all samples, the bands around 1453-1406 and 863  $\text{cm}^{-1}$ , associated with the  $\text{CO}_3^{2-}$  group [30, 43, 44], indicate that a certain proportion of carbonates from the reactants was incorporated into the apatitic structure. While the bands observed around 3444 and 1617  $\text{cm}^{-1}$  are attributable to molecular water adsorbed on the surface of the solid [45]. The allocation of absorption bands of the  $\text{PO}_4$  and  $\text{SiO}_4$  groups was carried out by comparison with the spectra of apatitic phases of similar compositions [26, 27, 41, 45, 46-49].

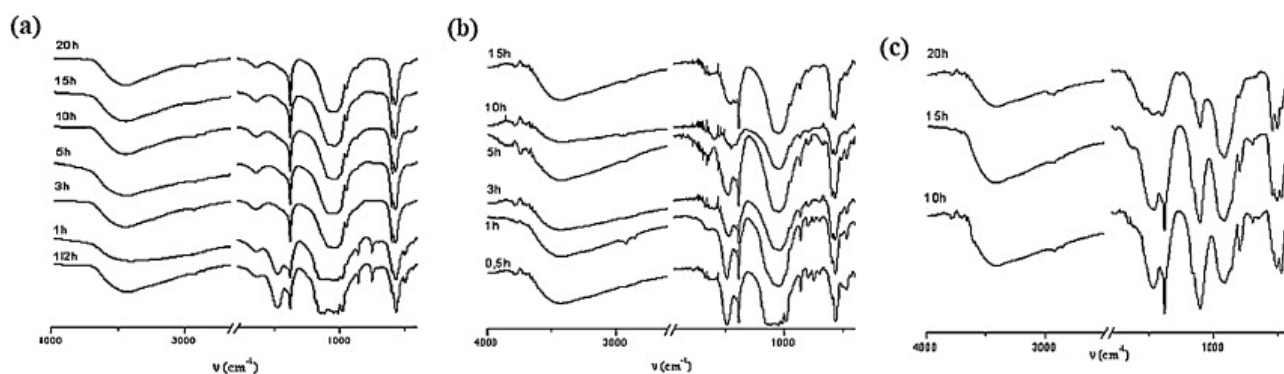


**Figure 8.** Infrared absorption spectra of crushed samples for periods between 30 minutes and 20 hours (**Eqn. 2**): (a):  $\text{Sr}_8\text{LaCs}$ ; (b):  $\text{Sr}_7\text{La}_2\text{Cs}$ ; (c):  $\text{Sr}_2\text{La}_7\text{Cs}$ .

For the  $\text{Sr}_8\text{LaCs}$  sample, after 30 minutes and one hour of grinding, the spectra show that the majority of the absorption bands belong to the reactants (**Figure 8a**). It is only from three o'clock that the formation of apatite becomes evident. The spectrum relative to this duration reveals the characteristic bands of  $(\text{PO}_4)_3^-$  groups in an apatitic environment. Thus, the bands located around 1079 and 1032  $\text{cm}^{-1}$  correspond to the asymmetrical elongations ( $\nu_3$ ), the band at 946  $\text{cm}^{-1}$  is related to the symmetrical elongations ( $\nu_1$ ) and the bands around 592 and 563  $\text{cm}^{-1}$  are relative to the asymmetrical deformations ( $\nu_4$ ). Note that the spectra remain practically identical up to 20 hours.

**Figure 8b** shows the infrared absorption spectra of the shredded  $\text{Sr}_7\text{La}_2\text{Cs}$  sample between 30 minutes and 15 hours. As with  $\text{Sr}_8\text{LaCs}$ , the absorption bands observed, for grinding times of 30 minutes and one hour, are relative to the reactants. For a period of three hours, the spectrum reveals, in addition to the absorption bands corresponding to the phosphate groups, bands associated with the silicate groups, detected around 916 ( $\nu_3$ ), 858 ( $\nu_1$ ) and 468 ( $\nu_4$ )  $\text{cm}^{-1}$ .

In addition to these bands, we note the presence of bands of low intensities around 799, 745 and 699  $\text{cm}^{-1}$  attributed to silica [55], not detected by DRX, probably because of its small amount. This unincorporated silica was replaced in the apatitic structure by carbonates from the reactants.

The spectra of the  $\text{Sr}_2\text{La}_7\text{Cs}$  sample, crushed for 10, 15 and 20 hours, shown in **Figure 8c** are typical of a silicate apatite. The shoulders detected around 900  $\text{cm}^{-1}$  are attributable to the symmetrical valence vibration mode ( $\nu_1$ ) of the  $\text{SiO}_4$  group. The bands positioned around 920, 500 and 540 and 420, 440 and 460  $\text{cm}^{-1}$  are, respectively, associated with the vibration modes  $\nu_3$ ,  $\nu_4$  and  $\nu_2$ . Similarly, for this silicate sample, we note the presence of bands of low intensities around 800, 722 and 698  $\text{cm}^{-1}$  attributable to silica [50].

### 3.4 Powders calcination

Samples prepared with strontium carbonate were calcined under argon atmosphere at 900°C for 12 hours after being crushed for 20 hours ( $\text{Sr}_8\text{LaCs}$  and  $\text{Sr}_7\text{La}_2\text{Cs}$ ) and five hours ( $\text{Sr}_2\text{La}_7\text{Cs}$ ) respectively. For the latter sample, this duration was chosen because of the absence of secondary phases in the crushed powder. The DRX spectra obtained are shown in **Figure 9**.

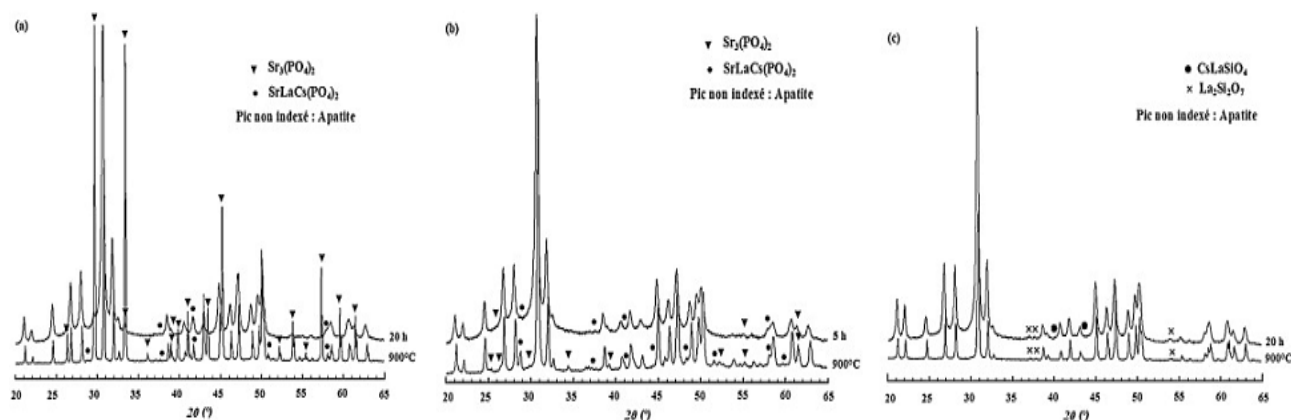


**Figure 9.** X-ray diffraction spectra of samples prepared according to **Eqn. 2** and calcined at 900 °C for 12 hours: **(a):**  $\text{Sr}_8\text{LaCs}$ ; **(b):**  $\text{Sr}_7\text{La}_2\text{Cs}$ ; **(c):**  $\text{Sr}_2\text{La}_7\text{Cs}$ .

For the  $\text{Sr}_8\text{LaCs}$  sample, **Figure 9a** suggests that during heat treatment, part of the apatite decomposed with the formation of tri-tructic phosphate. In crushed powder, its amount is very small compared to that of apatite, while after calcination, the DRX peaks of the two products are, respectively, of equal intensity. For the  $\text{SrLaCs}(\text{PO}_4)_2$  phase, we note only an improvement in its crystallinity. The decomposition of apatite should normally be accompanied by the formation of other phases, but these have not been detected. In the case of  $\text{Sr}_7\text{La}_2\text{Cs}$ , for grinding times of between three and five hours, the only phase detected is apatite. After heat treatment, the DRX spectrum reveals the presence in very small quantities of the  $\text{Sr}_3(\text{PO}_4)_2$  and  $\text{SrLaCs}(\text{PO}_4)_2$  phases (**Figure 9b**). As for the  $\text{Sr}_2\text{La}_7\text{Cs}$  sample, **Figure 9c** shows that the influence of calcination was only reflected in the improvement of the crystallinity of the powder, the proportions of the secondary phases,  $\text{La}_2\text{Si}_2\text{O}_7$  and  $\text{CsLaSiO}_4$ , having practically not varied.

Obtaining oxyapatite  $\text{La}_{9,33}(\text{SiO}_4)_6\text{O}_2$  by high temperature heat treatment is most often accompanied by the formation of the secondary phases  $\text{La}_2\text{SiO}_5$  and / or  $\text{La}_2\text{Si}_2\text{O}_7$  [50-52]. This last phase is formed in an amorphous state from 400°C and gradually crystallizes during the rise in temperature [53]. Once formed, it becomes almost impossible to remove it by calcination and obtain pure oxyapatite [54]. Vidal and Bernal [34] have shown that the mechanism of its formation is related to reactions on the surface of silica grains.

Therefore, it was possible for Béchade et al., [54] to prepare pure oxyapatite using very pure lanthanum oxide. Indeed, it is the hydrated lanthanum oxide that reacts with silica to give  $\text{La}_2\text{Si}_2\text{O}_7$ . It should be noted that Rodriguez-Reyna et al., were able to obtain pure oxyapatite by dry grinding of  $\text{La}_2\text{O}_3$  and  $\text{SiO}_2$  [55]. In the present work, we have observed the formation of  $\text{Sr}_3(\text{PO}_4)_2$ , whether the synthesis is carried out in one or two steps, and it remains present regardless of the grinding time. At high temperature (1400°C),  $\text{Sr}_3(\text{PO}_4)_2$  was also formed during the preparation of intermediate apatites, but it completely disappeared after the introduction of cesium in the second stage (1100°C)

[40]. It therefore seems that the operating conditions can be decisive in the formation of a given phase. However, experimental conditions alone cannot explain the difference observed in the nature of the secondary phases formed according to the two methods (present work and by heat treatment). Indeed, thermodynamic and/or kinetic considerations are surely behind this difference.

## Conclusion

Lacunary britholites with the general chemical formula  $\text{Sr}_{10-x}\text{La}_x(\text{PO}_4)_{6-x}(\text{SiO}_4)_x\text{F}_2$  with  $0 \leq x \leq 6$ , prepared by reaction in the solid state at 1400 °C. Also, these same products were prepared by mechano-synthesis, where the reactants were crushed in stoichiometric proportions for periods of between 30 minutes and 25 hours using a planetary mill.

X-ray diffraction and FTIR spectroscopy of the lacunar samples prepared by the two synthesis methods reveal the formation of secondary phases in addition to the majority apatitic phase. In the case of the compositions  $\text{Sr}_8\text{LaF}$  and  $\text{Sr}_7\text{La}_2\text{F}$ , the presence of secondary phases  $\text{Sr}_3\text{La}(\text{PO}_4)_3$  and  $\text{Sr}_3(\text{PO}_4)_2$  and in the case of the composition  $\text{Sr}_2\text{La}_7\text{F}$ , the secondary phases identified are  $\text{La}_2\text{Si}_2\text{O}_7$  and  $\text{La}_2\text{SiO}_5$ .

After incorporation of cesium, among the three intermediate compositions, only the composition  $\text{Sr}_7\text{La}_2\text{F}$  allows the obtaining of a pure apatitic phase of formula  $\text{Sr}_7\text{La}_2\text{Cs}(\text{PO}_4)_5(\text{SiO}_4)\text{F}_2$ . For the composition  $\text{Sr}_8\text{LaF}$ , there is disappearance of the secondary phases  $\text{Sr}_3\text{La}(\text{PO}_4)_3$  and  $\text{Sr}_3(\text{PO}_4)_2$  and the appearance of a new phase  $\text{SrLaCs}(\text{PO}_4)_2$ . In the case of the purely silicate lacunar phase treated with cesium, there is the presence of a majority apatitic phase of formula  $\text{Sr}_2\text{La}_7\text{Cs}(\text{SiO}_4)_6\text{F}_2$  and new secondary phases  $\text{CsLaSiO}_4$ ,  $\text{La}_2\text{Si}_2\text{O}_7$  and  $\text{Sr}_2\text{SiO}_4$ . The formation of these secondary phases suggests that the amount of cesium incorporated into apatite is lower than that initially introduced into mixtures.

## References

- [1] K. Sudarsanan, R.A. Youner, "Significant precision in crystal structural details: Holly springs hydroxyapatite", *Acta Crystallogr.*, B 25 (8) (1969) 1534.
- [2] G. Cannizzaro, P. Felice, M. Leone, P. Viola, M. Esposito, "Early loading of implants in the atrophic posterior maxilla: lateral sinus lift with autogenous bone and Bio-Oss versus crestal mini sinus lift and 8-mm hydroxyapatite-coated implants. A randomised controlled clinical trial", *Eur. J. Oral. Implantol.*, 2 (1) (2009) 25-38.
- [3] A. Stavropoulos, T. Karring, " Guided tissue regeneration combined with a deproteinized bovine bone mineral (Bio-Oss) in the treatment of intrabony periodontal defects: 6-year results from a randomized-controlled clinical trial", *J. Clin. Periodontol.*, 37 (2010) 200.
- [4] R.A. Yukna, P. Castellon, A.M. Saenz-Nasr, K. Owens, J. Simmons, K.H. Thunthy, E.T. Mayer, "Rietveld refinement, electronic structure and ionic conductivity of  $\text{Sr}_4\text{La}_6(\text{SiO}_4)_6\text{F}_2$  and  $\text{Sr}_4\text{La}_6(\text{SiO}_4)_6\text{O}$  ceramics", *J. Periodontol.*, 74 (2003) 679.
- [5] K.H. Butler, "Fluorescent Lamp Phosphors: Technology and Theory", The Pennsylvania State University Press, University Park, PA, 1980.
- [6] T. Welker, "Recent developments on phosphors for fluorescent lamps and cathode-ray tubes", *J. Lumin.* 48-49 (1991) 49.

- [7] J.P. Budin, J. C. Michel, F. Auzel, "Preparation, structure, optical, and magnetic properties of lanthanide aluminate single crystals ( $\text{LnMAI}_{11}\text{O}_{19}$ )", *J. Appl. Phys.* 50 (1979) 641.
- [8] Y. Matsumura, S. Sugiyama, H. Hayashi, J. B. Moffat, "The effects of the introduction of tetrachloromethane into the feedstream for the partial oxidation and oxidative coupling of methane", *J. Solid State Chem.* 114 (1995) 138.
- [9] L. Boyer, J. Carpena, J.L. Lacout, "Synthesis of phosphate-silicate apatites at atmospheric pressure", *J. Solid State Ionics* 95 (1997) 121.
- [10] R. Wallaëys, "Étude par diffraction des rayons X et par spectrométrie d'absorption infrarouge des apatites carbonatées de type A phospho-calcique et arsénio-calcique «haute pression»", *C.R. Coll. Intern. Chim. Pure et Appliquée, Münster, Westph.* (1954) 183.
- [11] E.R. Kreidler, "The crystal chemistry of apatite: structure fields of fluor- and chlorapatite", F.A. Hummel, *Am. Miner.* 55 (1970) 170.
- [12] R. El Ouenzerfi, C. Goutaudier, G. Panczer, B. Moine, M.T. Cohen-Adad, M. Trabelsi-Ayedi, N. Kbir-Arighuib, "Synthèse et caractérisation des phosphates silicatées", *J. Solid State Ionics* 156 (2003) 209.
- [13] J. Felsche, "Rare earth silicates with the apatite structure", *J. Solid State Chem.* (1972) 266.
- [14] C. Meis, "Computational study of plutonium–neodymium fluorobrotholite  $\text{Ca}_9\text{Nd}_{0.5}\text{Pu}_{0.5}(\text{SiO}_4)(\text{PO}_4)_5\text{F}_2$  thermodynamic properties and threshold displacement energies", *J. Nucl. Mater.* 289 (2001) 167.
- [15] C. Meis, J. D. Gale, L. Boyer, J. Carpena, D. Gosset, "Theoretical Study of Pu and Cs Incorporation in a Mono-silicate Neodymium Fluoroapatite  $\text{Ca}_9\text{Nd}(\text{SiO}_4)(\text{PO}_4)_5\text{F}_2$ ", *J. Phys. Chem.* 104 (2000) 5380.
- [16] L. Boyer, "Synthèses et caractérisations d'apatites phospho-silicatées aux terres rares : application au nucléaire", Doctoral Thesis, I.N.P. Toulouse (1998).
- [17] G.W. Wetherill, M.G. Inghram, "In Proceeding of Congress on Nuclear Processes in Geologic Settings", 21-23 September, 1953, p. 30.
- [18] R. Bros, J. Carpena, V. Sere, A. Beltritti, *Radiochim.*, "Occurrence of Pu and Fissionogenic REE in Hydrothermal Apatites from the Fossil Nuclear Reactor 16 at Oklo (Gabon)", *Acta* 74 (1996) 277.
- [19] H. Arikawa, H. Nishiguchi, T. Ishihara, Y. Takita, "Oxide ion conductivity in Sr-doped  $\text{La}_{10}\text{Ge}_6\text{O}_{27}$  apatite oxide", *Solid State Ionics* 136-137 (2000) 31.
- [20] S. Nakayama, M. Sakamoto, "Electrical properties of new type high oxide ionic conductor  $\text{RE}_{10}\text{Si}_6\text{O}_{27}$  (RE= La, Pr, Nd, Sm, Gd, Dy)", *J. Eur. Ceram. Soc.* 18 (1998) 1413.
- [21] S. Nakayama, H. Aono, Y. Sadaoka, "Ionic Conductivity of  $\text{Ln}_{10}(\text{SiO}_4)_6\text{O}_3$  (Ln = La, Nd, Sm, Gd and Dy)", *Chem. Lett.* 6 (1995) 431.
- [22] L. W. Schroeder, M. Mathew, "Cation ordering in  $\text{Ca}_2\text{La}_8(\text{SiO}_4)_6\text{O}_2$ ", *J. Solid State Chem.* 26 (1978) 383.
- [23] S. Nakayama, T. Kageyama, H. Aono, Y. Sadaoka, "Ionic conductivity of lanthanoid silicates,  $\text{Ln}_{10}(\text{SiO}_4)_6\text{O}_3$  (Ln= La, Nd, Sm, Gd, Dy, Y, Ho, Er and Yb)", *J. Mater. Chem.* 5 (1995) 1801-1805.
- [24] L. Boyer, J. Carpena, J.-L. Lacout, "Synthesis of phosphate-silicate apatites at atmospheric pressure", *Solid State Ionics* 95 (1997) 12.
- [25] K. Boughzala, E. Ben Salem, A. Ben Chrifa, E. Gaudin, K. Bouzouita, "Synthesis and characterization of strontium–lanthanum apatites", *J. Mater. Res. Bull.* 42 (2007) 1221.

- [26] O. Terra, N. Dacheux, F. Audubert, R. Podor, "Immobilization of tetravalent actinides in phosphate ceramics", *J. Nucl. Mater.* 352 (2006) 224.
- [27] O. Terra, F. Audubert, N. Dacheux, C. Guy, R. Podor, "Synthesis and characterization of uranium-bearing britholites", *J. Nucl. Mater.* 366 (2007) 70.
- [28] A.E. Yermakov, E.E. Yurchikov, V.A. Barinov, " The magnetic properties of amorphous Y-Co alloy powders obtained by mechanical comminution", *J. Phys. Met. Metallogr.* 52 (1981) 50.
- [29] C.C. Koch, O.B. Cavin, C.G. Mekamey, J.O. Scarbrough, " Preparation of "amorphous" Ni<sub>60</sub>Nb<sub>40</sub> by mechanical alloying", *J. Appl. Phys. Lett.* 43 (11) (1983) 1017.
- [30] N. Gmati, K. Boughzala, M. Abdellaoui, K. Bouzouita, " Mechanochemical synthesis of strontium britholites: Reaction mechanism", *C. R. Chimie* 14 (2011) 896.
- [31] N. Gmati, K. Boughzala, A. Chaabène, N. Fattah, K. Bouzouita, " Mechano-chemical synthesis of strontium apatites doped with lanthanum and cesium", *C. R. Chimie* 16 (2013) 712.
- [32] J.S. Benjamin, " Dispersion strengthened aluminum made by mechanical alloying", *Metall. Trans* 1 (1970) 2943.
- [33] M. Abdellaoui, E. Gaffet, " The physics of mechanical alloying in a planetary ball mill: mathematical treatment", *Acta Metall. Mater.* 43 (1995) 1087.
- [34] M. Abdellaoui, E. Gaffet, " A mathematical and experimental dynamical phase diagram for ball-milled Ni<sub>10</sub>Zr<sub>7</sub>", *J. Alloys Compd.* 209 (1994) 351.
- [35] N. Senamaud, " Synthesis and characterization of Cs-bearing apatites", thèse de doctorat, Limoges, France, 1999.
- [36] R.D. Shannon, " Revised effective ionic radii and systematic studies of interatomic distances in halides and chalcogenides", *Acta Crystallogr. A* 32 (1976) 751.
- [37] L. Campayo, Thèse de Doctorat, " Incorporation du césium dans des phosphates de structure apatitique et rhabdophane : Application au conditionnement des radionucléides séparés", Limoges, France, 2003.
- [38] L. Campayo, F. Audubert, D. Bernache-Assollant, "Synthesis study of alkaline-bearing rare earth phosphates with rhabdophane structure " *J. Solid State Ionics* 176 (2005) 663.
- [39] N. Senamaud, D. Bernache-Assollant, J. Carpena, M. Fialin, "Cesium incorporation into phosphate silicate apatites". *Phosphorus Res. Bull.* 10 (1999) 353.
- [40] K. Boughzala, M. Hidouri, E. Ben Salem, A. Ben Chrifa, K. Bouzouita, " Insertion du césium dans des britholites au strontium", *C. R. Chimie* 10 (2007) 1137.
- [41] K. Boughzala, E. Ben Salem, A. Ben Chrifa, E. Gaudin, K. Bouzouita, "Synthesis and characterization of strontium–lanthanum apatites", *Mater. Res. Bull.* 42 (2007) 1221.
- [42] A. Aissa, B. Badraoui, R. Thouvenot, M. Debbabi, "Synthesis, X-ray Structural Analysis and Spectroscopic Investigations (IR and <sup>31</sup>P MAS NMR) of Mixed Barium/Strontium Fluoroapatites", *Eur. J. Inorg. Chem.* 3228 (2004).
- [43] H.E. Feki, J.M. Savariault, A. Ben Salah, " Structure refinements by the Rietveld method of partially substituted hydroxyapatite: Ca<sub>9</sub>Na<sub>0.5</sub>(PO<sub>4</sub>)<sub>4.5</sub>(CO<sub>3</sub>)<sub>1.5</sub>(OH)<sub>2</sub>", *J. Alloys Compd.* 287 (1999) 114.
- [44] J.P. Lafon, E. Champion, D. Bernache-Assollant, " Processing of AB-type carbonated hydroxyapatite Ca<sub>10-x</sub>(PO<sub>4</sub>)<sub>6-x</sub>(CO<sub>3</sub>)<sub>x</sub>(OH)<sub>2-x-2y</sub>(CO<sub>3</sub>)<sub>y</sub> ceramics with controlled composition", *J. Eur. Ceram. Soc.* 28 (2008) 139.

- [45] Khorari S, Cahay R, Rulmont A, Tarte P., " The coupled isomorphic substitution  $2(\text{PO}_4)^{3-}(\text{SO}_4)^{2-}+(\text{SiO}_4)^{4-}$  in synthetic apatite  $\text{Ca}_{10}(\text{PO}_4)_6\text{F}_2$ : a study by X-ray diffraction and vibrational spectroscopy", *Eur. J. Solid State Chem.* 31 (1994) 921.
- [46] O. Terra, F. Audubert, N. Dacheux, C. Guy, R. Podor, J. Nucl. " Synthesis and characterization of thorium-bearing britholites", *Mater.* 354 (1-3) (2006) 49-65.
- [47] N. Dacheux, E. Du Fou De Kerdaniel, N. Clavier, R. Podor, J. Aupiais, " Kinetics of dissolution of thorium and uranium doped britholite ceramics", *J. Nucl. Mater.* 404 (2010) 33.
- [48] B.O. Fowler, " Infrared studies of apatites. I. Vibrational assignments for calcium, strontium, and barium hydroxyapatites utilizing isotopic substitution", *Inorg. Chem.* 13 (1) (1974) 194.
- [49] J. Neubauer, H. Pollmann, "Solid-Solution series of silico-sulfate-chloride-apatites", *N. Jahrb, Mineral. Abh.* 168 (3) (1995) 237.
- [50] G. Tzvetkov, N. Minkova, " Mechanochemical stimulation of the synthesis of lanthanum oxyapatite", *Mater. Lett.* 39 (1999) 354.
- [51] A.F. Fuentes, E. Rodriguez-Reyna, L.G. Martinez-Gonzalez, M. Maczka, J. Hamuza, U. Amador, "Room-temperature synthesis of apatite-type lanthanum silicates by mechanically milling constituent oxides", *Solid State Ionics* 177 (2006) 1869.
- [52] A. Christensen, R.G. Hazell, A.W. Hewat, "Synthesis, crystal growth and structure investigations of rare-earth disilicates and rare-earth oxyapatites", *Acta Chem. Scand.* 51 (1997) 37.
- [53] D.J. Lichtenwalner, J.S. Jur, A.I. Kingon, M.P. Agustin, Y. Yang, S. Stemmer, L.V. Goncharova, T. Gustafsson, E. Garfunkel, "Lanthanum silicate gate dielectric stacks with subnanometer equivalent oxide thickness utilizing an interfacial silica consumption reaction", *J. Appl. Phys.* 98 (2005).
- [54] E. Béchade, I. Julien, T. Iwata, O. Masson, P. Thomas, E. Champion, K. Fukuda, Synthesis of lanthanum silicate oxyapatite materials as a solid oxide fuel cell electrolyte, *J. Eur. Ceram. Soc.* 28 (2008) 2717-2724.
- [55] E. Rodriguez-Reyna, A.F. Fuentes, M. Maczka, J. Hanuza, K. Boulahya, U. Amador, " Structural, microstructural and vibrational characterization of apatite-type lanthanum silicates prepared by mechanical milling", *J. Solid State Chem.* 179 (2006) 522.

(2022) ; <http://www.jmaterenvironsci.com>